

Gas on the Virgo cluster from WMAP and ROSAT observations

Jose M. Diego, Yago Ascasibar

Abstract WMAP observations at mm wavelengths are sensitive to the Sunyaev-Zel'dovich effect in galaxy clusters. Among all the objects in the sky, the Virgo cluster is expected to provide the largest integrated signal. Based on models compatible with the X-ray emission observed in the ROSAT All Sky Survey, we predict an approximately two-sigma detection of the SZ effect from Virgo in the WMAP 3-year data. Our analysis reveals a 3-sigma signal on scales of 5 degrees, although the frequency dependence deviates from the theoretical expectation for the SZ effect. The main sources of uncertainty are instrumental noise, and most importantly, possible contamination from point sources and diffuse back/foregrounds.

1 Introduction

The X-ray emission and the Sunyaev-Zel'dovich (SZ) effect provide complementary probes of the physical state of the hot intracluster medium (ICM). In galaxy clusters, the dominant mechanism for X-ray emission is thermal bremsstrahlung, and the surface brightness is roughly proportional to the integral along the line of sight of the gas density squared [26]. The SZ effect, on the other hand, is proportional to the integrated energy density of the electrons, i.e. the gas pressure [30, 8]. In general, there is good agreement between estimates of the gas density based on X-ray and interferometric radio data, at least within the central regions accessible to both types of observation. Such agreement has also been reported at millimeter wavelengths, although the results seem to indicate a baryon fraction that is considerably lower than the cosmic value [2, 1, 23]. While this would be perfectly consistent with

Jose M. Diego
IFCA, Universidad de Cantabria-CSIC, 39005 Santander, e-mail: jdiego@ifca.unican.es

Yago Ascasibar
Astrophysikalisches Institut Potsdam, Germany & Universidad Autonoma de Madrid. e-mail: yago.ascasibar@uam.es

measurements based on X-ray observations only [14, 25, 3, 12, 32] as well as theoretical estimates of the baryon fraction expected in the central regions of the ICM [6, 5, 19, 13], recent studies based on WMAP data have suggested that the SZ effect observed in galaxy clusters might actually be weaker than one would infer from their X-ray luminosity [20, 7]. The presence of point sources could compensate part of the SZ temperature decrement at WMAP frequencies, but the required flux would be much higher than the observational upper limits [11, 22]. An interesting alternative explanation would be that a non-thermal population of relativistic electrons promoted CMB photons into the X-ray regime by inverse Compton scattering [21]. In this scenario, the gas density required to produce the observed X-ray flux would be lower than for a thermalized plasma, and the corresponding SZ effect would be dimmer. In this paper we address the question of whether the SZ effect detected in WMAP-3yr data is compatible with the observed X-ray emission. We focus on the brightest and most extended source in the sky at both wavelengths: the Virgo cluster. Due to its small distance from us and its relatively large mass, the integrated SZ flux from Virgo must be larger than that from any other cluster [31]. This object has also the largest integrated X-ray flux, as can be clearly seen, for instance, in the data from the ROSAT All Sky Survey. Here we investigate two different models of the intracluster medium that are consistent with the observed X-ray emission from Virgo, and we predict their expected SZ effect in WMAP data.

2 WMAP and ROSAT Data

Notwithstanding its large integrated X-ray flux, which made possible its detection by the *Einstein* [15] and *Ginga* [18] satellites, the large angular extent of the Virgo cluster, about 6° in radius, prevented the elaboration of high-resolution maps until the data from the ROSAT All Sky Survey (RASS) became available. The X-ray surface brightness was found to be strongly peaked at the location of M87, and the large-scale morphology of the ICM traces the galaxy distribution, with three major sub-clusters centered around M87, M86, and M49 [9, 27]. The Virgo cluster has also been observed by more recent X-ray observatories, such as *Chandra* and *XMM-Newton*, but these instruments feature a narrower field of view [10, 33], and the new data is restricted to very small regions within the cluster. Since we are interested on much larger scales, our work is based on the RASS maps of the diffuse X-ray emission [29].

At this stage, the map still seems at first sight to be completely dominated by instrumental noise. However, this component can be well described by white Gaussian noise, and therefore its magnitude can be reduced by averaging over a large area. As long as we do not exceed the scale of the cluster, the SZ signal from Virgo will be enhanced by this process, because the amplitude of the noise (the dispersion around the average, which is 0) decreases as the square root of the number of pixels involved, or, equivalently, the characteristic length of the smoothing kernel. The result obtained after excluding point sources and filtering out the noise with a

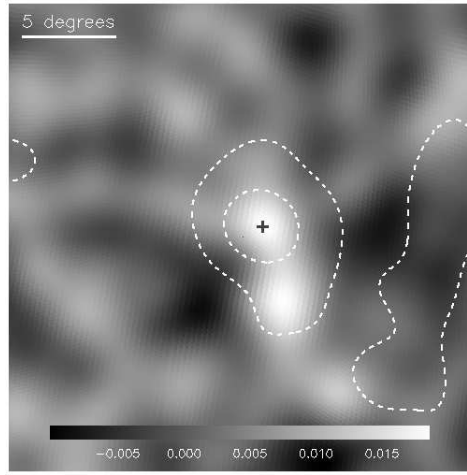
Gaussian of $\text{FWHM} = 3^\circ$ can be seen in Figure 1. There is a positive fluctuation at the center, as expected for the SZ effect. This signal seems to extend a few degrees south, apparently correlated with the X-ray emission. It could be a genuine SZ signature, but also a fluctuation of the noisy background or even a contribution from unresolved sources with a SZ-like spectrum (like dusty galaxies).

3 Analysis

The ROSAT X-ray emission (up to ~ 5 degrees) is used to set the values of the model parameters. The first model is based on [4] (AD08) and the second one in [16] (G04). We employ a particle swarm optimization algorithm to fit the ROSAT data in the four bands simultaneously. At large distances, G04 assume a constant temperature of 2.4 keV, while the ICM gas in the AD08 model reaches values up to ~ 4 keV and then drops towards larger radii. Although the X-ray emission is almost identical in both models the exact temperature of the most distant regions can be relevant for the SZ effect. The temperature profile of the Virgo cluster at large radii has not been determined accurately. ASCA measurements between M87 and M49 [28] show a maximum temperature of 4 keV in a low density region about three degrees (~ 900 kpc) south of M87. In this sense, the temperature predicted by the AD08 model could provide a better description of distant low-density regions that are not bright enough to be seen in the ROSAT data.

Given a model of the ICM, it is straightforward to predict the expected SZ signal, but the comparison with WMAP data is far from simple. As opposed to X-rays, it is not possible to see Virgo directly in WMAP because the SZ effect is weaker than the underlying CMB. We consider a region of $25.65^\circ \times 25.65^\circ$ around the location of M87, extracted from the WMAP-3yr data set [17]. To reduce the CMB contamination, we perform a basic cleaning process that makes use of the well-known frequency independence of the CMB anisotropies. We consider the foreground-reduced maps in the Q, V, and W bands, corresponding to frequencies of 41, 61, and 94 GHz, respectively. The angular resolution of these bands are 0.51° , 0.35° , and 0.22° respectively. The Foreground Template Model discussed in [17] and [24] has been subtracted from all the unreduced sky maps. A simple linear combination of the WMAP channels can produce a new map where the CMB vanishes, at the expense of removing a significant fraction of the SZ signal and increasing the noise level. Also, the resolution of the V and W channels must be degraded to match that of the Q channel. Our choice, $V+W-2Q$, tries to maximize the SZ residual. Due to the frequency dependence of the SZ effect, this combination has positive sign in those areas where the SZ effect is dominant with respect to other sources. From now on we will refer to the linear combination $V+W-2Q$ as the *residual SZ map*. Unfortunately, the CMB is not the only contaminant that must be dealt with. As will be discussed in more detail later, there is also contamination by point sources and diffuse emission of different kinds. The residual SZ map still seems at first sight to be completely dominated by instrumental noise. However, this component can be well

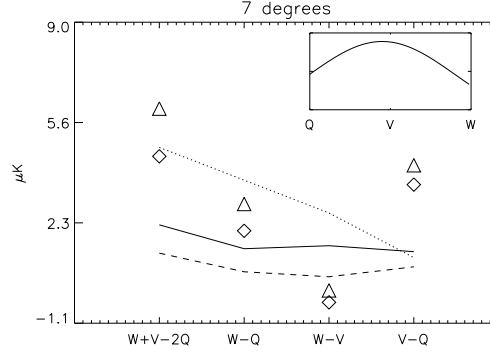
Fig. 1 3 degree smoothed WMAP residual ($V + W - 2Q$). Contours show the Virgo region (smoothed with a 3 degree fwhm Gaussian) as seen by ROSAT in the R6 band (0.9 – 1.3 keV). The structure to the right of Virgo in ROSAT data is diffuse emission from the Galaxy. The black cross in the center marks the position of the central galaxy M87 (it has been masked out in this plot). In this and the other plots, the field of view is 25.65 degrees on a side and centered on Virgo. The colorbar shows the scale in mili Kelvin.



described by white Gaussian noise, and therefore its magnitude can be reduced by averaging over a large area. As long as we do not exceed the scale of the cluster, the SZ signal from Virgo will be enhanced by this process, because the amplitude of the noise (the dispersion around the average, which is 0) decreases as the square root of the number of pixels involved, or, equivalently, the characteristic length of the smoothing kernel. The result obtained after excluding point sources and filtering out the noise with a Gaussian of FWHM= 3° can be seen in Figure 1. There is a positive fluctuation at the center, as expected for the SZ effect. This signal seems to extend a few degrees south, apparently correlated with the X-ray emission. It could be a genuine SZ signature, but also a fluctuation of the noisy background or even a contribution from unresolved sources with a SZ-like spectrum (like dusty galaxies). Interestingly, the mean intensity of the residual SZ map deviates significantly from zero. Such deviation is neither compatible with the expected mean SZ signal from Virgo nor with a large scale fluctuation of the Gaussian noise.

A mere visual inspection of Figure 1 indicates that there is indeed a positive fluctuation in the residual SZ map at the position of the Virgo cluster. It is our goal to find out whether the signal constitutes a statistically significant detection, or it can be understood as a random fluctuation of the instrumental noise. Also we want to check whether it is compatible or not with the expectation from the models based on X-ray data. We can address both questions by computing the probability that the measured intensity arises from pure Gaussian random noise, and compare it with another process in which the average equals the expected SZ signal. To compute these probabilities, we carried out Monte Carlo simulations based on our analytical model, G04, and the null hypothesis. All of them involve the addition of fake instrumental noise, application of the point source mask, and Gaussian smoothing, mimicking the analysis of the real WMAP data. We account for the random noise by generating 400 realizations using the published sensitivity per channel and the

Fig. 2 Observed versus predicted signal for the different combination of channels (after smoothing with a 7 degree FWHM Gaussian). The triangles show the observed signal in the different combinations (clean data). The diamonds is the same but for uncleaned WMAP data. The dotted line shows the predicted SZ signal. Dashed line shows the predicted RMS of the background of non-removed non-clustered radio sources and the solid line shows the expected RMS of the instrumental noise.



number of observations per pixel. A realization of the noise is made for each of the 8 channels involved (Q1,Q2,V1,V2,W1,W2,W3, and W4). These channels are combined to produce the Q, V, and W maps. The resulting V and W maps are then degraded to the resolution of Q, and the linear combination $V+W-2Q$ is constructed.

To these simulated noise maps we add the predicted SZ effect from Virgo, according to our two different models. The WMAP point source mask is then applied, and the map is convolved with a Gaussian filter of 5 degrees FWHM. We found that on average the models predict a 2σ fluctuation which is comparable to the observed 2σ fluctuation. Alternative analyses based on the distribution of the maxima in the simulated data and their probability density function also indicate that the observed fluctuation is compatible with the existence of the expected SZ signal derived from X-ray observations.

4 Unexpected Results

Two surprises were found when analyzing the data. When taking the average of the considered region this one deviates significantly from zero (7σ). Some of the foreground Galactic components could leave a residual in this region if they are not properly removed. Other possibility is non-removed extragalactic point sources which also could leave a residual in the $V+W-2Q$ map if they are clustered. The other surprise appears when we look at the frequency dependence of the fluctuation in all the possible differences. The residual shows the expected dust-like spectrum between the Q and V channels but between V and W the spectrum is similar to a synchrotron dominated one (see figure 2). This could be an indication of possible contamination in this region of the sky either from Galactic or extragalactic sources.

Acknowledgements This work has been funded by the Spanish *Ministerio de Educación y Ciencia*, project AYA2006-06266, and JMD benefits from a contract under the *Ramón y Cajal* programme.

References

1. Afshordi N., Lin Y.-T., Nagai D., Sanderson A. J. R., 2007, MNRAS, 378, 293
2. Afshordi N., Lin Y.-T., Sanderson A. J. R., 2005, ApJ, 629, 1
3. Allen S. W., Schmidt R. W., Fabian A. C., 2002, MNRAS, 334, L11
4. Ascasibar Y., Diego J. M., 2008, MNRAS, 383, 369
5. Ascasibar Y., Sevilla R., Yepes G., Müller V., Gottlöber S., 2006, MNRAS, 371, 193
6. Ascasibar Y., Yepes G., Müller V., Gottlöber S., 2003, MNRAS, 346, 731
7. Bielby R. M., Shanks T., 2007, ArXiv Astrophysics e-prints
8. Birkinshaw M., 1999, Phys. Rep., 310, 97
9. Bohringer H., Briel U. G., Schwarz R. A., Voges W., Hartner G., Trumper J., 1994, Nature, 368, 828
10. Bohringer H., Belsole E., Kennea J., Matsushita K., Molendi S., Worrall D. M., Mushotzky R. F., Ehle M., Guainazzi M., Sakellou I., Stewart G., Vestrand W. T., Dos Santos S., 2001, A&A, 365, L181.
11. Coble K., Bonamente M., Carlstrom J. E., Dawson K., Hasler N., Holzapfel W., Joy M., LaRoque S., Marrone D. P., Reese E. D., 2007, AJ, 134, 897
12. Etti S., 2003, MNRAS, 344, L13
13. Etti S., Dolag K., Borgani S., Murante G., 2006, MNRAS, 365, 1021
14. Etti S., Fabian A. C., 1999, MNRAS, 305, 834
15. Fabricant D., Gorenstein P., 1983, ApJ, 267, 535
16. Ghizzardi S., Molendi S., Pizzolato F., De Grandi S., 2004, ApJ, 609, 638
17. Hinshaw G., Nolte M. R., Bennett C. L., et al. 2007, ApJS, 170, 288
18. Koyama K., Takano S., Tawara Y., 1991, Nature, 350, 135
19. Kravtsov A. V., Nagai D., Vikhlinin A. A., 2005, ApJ, 625, 588
20. Lieu R., Mittaz J. P. D., Zhang S.-N., 2006, ApJ, 648, 176
21. Lieu R., Quenby J., 2006, ArXiv Astrophysics e-prints
22. Lin Y.-T., Mohr J. J., 2007, ApJS, 170, 71
23. McCarthy I. G., Bower R. G., Balogh M. L., 2007, MNRAS, 377, 1457
24. Page L., Hinshaw G., Komatsu E., et al. 2007, ApJS, 170, 335
25. Roussel H., Sadat R., Blanchard A., 2000, A&A, 361, 429
26. Sarazin C. L., 1986, Reviews of Modern Physics, 58, 1
27. Schindler S., Bingeli B., Böhringer H., 1999, A&A, 343, 420
28. Shibata R., Matsushita K., Yamasaki N. Y., Ohashi T., Ishida M., Kikuchi K., Bohringer H., Matsumoto H., 2001, ApJ, 549, 228.
29. Snowden S. L., Egger R., Freyberg M. J., McCammon D., Plucinsky P. P., Sanders W. T., Schmitt J. H. M. M., Truemper J., Voges W., 1997, ApJ, 485, 125
30. Sunyaev R.A., Zeldovich Y.B., 1972, Comments on Astrophysics and Space Physics, 4, 173.
31. Taylor J. E., Moodley K., Diego J. M., 2003, MNRAS, 345, 1127
32. Vikhlinin A., Kravtsov A., Forman W., Jones C., Markevitch M., Murray S. S., Van Speybroeck L., 2006, ApJ, 640, 691
33. Young A. J., Wilson A. S., Mundell C. G., 2002, ApJ, 579, 560.